Title

Exosome Released From Schwann Cells May Be Involved in Microenergy Acoustic Pulse–Associated Cavernous Nerve Regeneration

Journal

The Journal of Sexual Medicine, 17(9)

ISSN

1743-6095

Authors

Peng, Dongyi
Reed-Maldonado, Amanda B
Zhou, Feng
et al.

Publication Date

2020-09-01

DOI

10.1016/j.jsxm.2020.05.018

Peer reviewed

HHS Public Access

Author manuscript

J Sex Med. Author manuscript; available in PMC 2021 September 01.

Published in final edited form as:

J Sex Med. 2020 September ; 17(9): 1618–1628. doi:10.1016/j.jsxm.2020.05.018.

Exosome Released from Schwann Cells May be Involved in MAP-associated Cavernous Nerve Regeneration

Dongyi Peng[1,2], **Amanda B. Reed-Maldonado**[1], **Feng Zhou**[1], **Yan Tan**[1], **Huixing Yuan**[1], **Lia Banie**[1], **Guifang Wang**[1], **Yuxin Tang**[3], **Leye He**[2], **Guiting Lin**[1], **Tom F. Lue**[1,*]

[1]Knuppe Molecular Urology Laboratory, Department of Urology, School of Medicine, University of California, San Francisco, CA 94143, USA

[2]Department of Urology, Third Xiangya Hospital of Central South University, Changsha 410013, China

[3]Department of Urology, Fifth Affiliated Hospital of Sun Yat-sen University, Zhuhai 519000, China

Abstract

Background—Neurogenic erectile dysfunction (ED) is often refractory to treatment due to insufficient functional nerve recovery after injury or insult. Noninvasive mechano-biological intervention, such as microenergy acoustic pulse (MAP), low-intensity pulsed ultrasound (LIPUS), and low-intensity extracorporeal shockwave treatment (Li-ESWT), is an optimal approach to stimulate nerve regeneration.

Aim—To establish a new model *in vitro* to simulate nerve injury in neurogenic ED and to explore the mechanisms of MAP *in vitro*.

Methods—Sprague-Dawley rats were used to isolate Schwann cells (SCs), major pelvic ganglion (MPG), and cavernous nerve with MPG (CN/MPG). SCs were then treated with MAP (0.033 mJ/mm^2, 1Hz, 100 pulses), and SC exosomes were isolated. The MPG and CN/MPG were treated with MAP (0.033 mJ/mm^2, 1 Hz) at different dosages (25, 50, 100, 200, or 300 pulses) or exosomes derived from MAP-treated SCs *in vitro*.

Outcomes—Neurite growth from the MPG fragments and CN was photographed and measured. Expression of neurotropic factors (BDNF, NGF, and NT-3) was checked.

Results—Neurite outgrowth from MPG and CN/MPG was enhanced by MAP in a dosage response manner, peaking at 100 pulses. MAP promoted SC proliferation, neurotropic factor (BDNF, NGF and NT-3) expression, and exosome secretion. SC-derived exosomes significantly enhanced neurite outgrowth from MPG *in vitro*.

Clinical Implications—MAP may have utility in the treatment of neurogenic ED by SC-derived exosomes.

*Corresponding Author: Tom F. Lue, MD, Department of Urology, University of California, San Francisco, 400 Parnassus Ave., Ste A-630, San Francisco, CA 94143-0738, USA, Phone (O): 415-4761611, Fax: 415-476 3803, tom.lue@ucsf.edu.

Strength & Limitations—We confirmed that MAP enhance penile nerve regeneration through exsomes. Limitations of this study include that our study did not explore the exact mechanisms of how MAP increases SC exosome secretion nor whether MAP modulates the content of exosomes.

Conclusion—This study revealed that neurite outgrowth from MPG was enhanced by MAP and by SC-derived exosomes which were isolated after MAP treatment. Our findings indicate that one mechanism by which MAP induces nerve regeneration is by stimulation of SCs to secrete exosomes.

INTRODUCTION

Since introduction in the late 1990s, the phosphodiesterase type-5 inhibitors have had a tremendous positive effect on the treatment of erectile dysfunction (ED). Additional medical treatment options for ED include intracavernous penile injections, medicated urethral suppositories, and testosterone replacement in men with ED and hypogonadism. Nevertheless, men who have nerve damage consequent to trauma or surgery are often refractory to these medical therapies. In many cases these patients must resort to surgery for penile prosthesis implantation to regain potency. Neurogenic ED, defined as the inability to achieve and maintain a penile erection due to central or peripheral nerve damage or both[1], is a clinical challenge due to the insufficient functional repair capacity of damaged nerves[2–4]. For this patient population, a novel therapy to prevent the deterioration of erectile function secondary to nerve damage is desperately needed.

Many methods have been explored with the goal of stimulating nerve regeneration, but these methods have shown modest benefit. These methods include exposure to specific external physical stimuli (magnetic fields[5], lasers[6], electrical impulses[7]) and application of biological therapies (neurotrophic factors[8], vitamins[9], medications[10]). More recently, mechano-biological interventions, such as low-intensity extracorporeal shockwave treatment (Li-ESWT), have been successfully utilized in the field of regenerative medicine. Research has shown that Li-ESWT can promote peripheral nerve regeneration after injury by activating Schwann cells (SCs) and by promoting SCs to secrete neurotropic factors[11,12]. The therapeutic effects of Li-ESWT in ED have been attributed to the stimulation of cell proliferation, tissue regeneration, and angiogenesis [13–16]. Moreover, studies have investigated the effects of Li-ESWT in the treatment of neurogenic ED specifically and have shown considerable promise[17,18]. In 2016, a pilot study by Frey *et al.* [18] found that Li-ESWT might ameliorate erectile function significantly in patients who had undergone robot-assisted bilateral nerve-sparing radical prostatectomy and suffered from mild to severe postoperative ED for more than one year. Also in 2016, Li *et al.*[19] employed a rat pelvic neurovascular injury model and demonstrated that Li-ESWT promotes nerve regeneration in neurogenic ED through activation of SCs.

Peripheral nerve regeneration after injury relies on both injured axons and non-neuronal cells. These non-neuronal cells include SCs, endoneurial fibroblasts, and macrophages; together these cells produce a supportive microenvironment allowing for successful regrowth of the proximal nerve fiber ending[20]. The composition of the cavernous nerve (CN) is unique as Schaumburg and associates reported numerous ganglion cells in the initial

segments, and the nerve contains both myelinated and unmyelinated nerve fibers[21]. The number of myelinated fibers gradually decreases distally, and at the point of crural entry, the CN contains almost exclusively unmyelinated axons.

SCs play a particularly important role in nerve regeneration after injury in the PNS[22–26]. SCs secret chemokines for the recruitment of circulating macrophages [27,28], produce neurite-promoting proteins [29], and express neurotrophic factors[20] to regulate peripheral nerve regeneration. In a previous study, our laboratory demonstrated that SCs enhance nerve regeneration through the Jak/STAT pathway[30] and that Li-ESWT promotes brain-derived neurotrophic factor (BDNF) secretion from SCs through the PERK pathway[31]. More recently, studies showed that SC-derived exosomes can enhance axonal regeneration and improve neuronal survival after nerve damage[32–34]. Exosomes are 40–200nm vesicles that function in the transfer of macromolecules between cells, and they play an important role in mediating intercellular communication in the nervous system. Exosomes contain microRNA and proteins which are involved in various key processes during nerve regeneration [35,36].

We have studied the biology of Li-ESWT[37], and demonstrated that the focused Li-ESWT devices currently on the market are not the best approaches for ED treatment because the energy flux density transmitted by these devices is excessive. In fact, these devices are potentially harmful to penile stem/progenitor cells [19143839]. Very recently, we have developed a new technology and named “microenergy acoustic pulse (MAP)” and successfully applied [40].

In this study, we aimed to develop a better model to simulate nerve regeneration in vitro and to explore the mechanisms of MAP *in vitro*.

MATERIALS and METHODS

Animals

All rats were obtained from Charles River Laboratories (Wilmington, MA, USA). The animal care and experimental procedures were approved by the Institutional Animal Care and Use Committee at the University of California, San Francisco. Sixteen male Sprague Dawley (SD) adult rats at age 12 weeks old were used in this study. All animals were kept in 12/12 hours light/dark cycle lighting with food and water available.

Major pelvic ganglion (MPG) and CN/MPG Culture

Bilateral CN/MPG (entire MPG with a 2mm length CN attached) complexes from each rat were isolated and excised intact (anatomy of CN and MPG shown in Fig. 2a). Each CN/MPG complex was placed in a glass-covered six-well plate then covered with 40μL of growth factor-reduced Corning Matrigel (Fisher Scientific) as previously described [4142,43]. In separate experiments, MPG without CN were isolated and rinsed in PBS. Each isolated MPG was further dissected to isolate the dorsocaudal region (DCR) of the MPG. This was then divided into three pieces of similar size and placed in a glass-covered six-well plate covered with 40μL Matrigel[4142] After incubation at 37°C for 5 minutes, either 3.0ml_ of complete DMEM medium without FBS or 3.0mL of complete DMEM medium with 500μL of SC-derived exosomes was added according to grouping.

SC Isolation and Culture

Primary SCs were isolated from the 6 SD rat sciatic nerve and were maintained in DMEM with 10% FBS in a humidified 5% C02, 37°C incubator as previously reported[44]. Identification of SCs was conducted with immunofluorescence (IF) staining with S-100 (Dako, Santa Clara, CA) and myelin basic protein (MBP) (Abeam, Cambridge, UK).

MAP Treatment

We used the MAP system to treat MPG and MPG/CN as shown in Fig 3a. The 36 MPG fragments from 6 adult SD rats were equally divided into 6 groups and treated with MAP (0.033mJ/mm^2, 1 Hz) at 6 different dosages (0, 25, 50, 100, 200, 300 pulses) twice (2 hours and 24 hours after seeding). Neurite growth was measured at 72 hours after seeding. The 16 CN/MPG from another 6 SD adult rats were either treated with MAP (0.033mJ/mm^2, 1 Hz, 100 pulses) twice (2 hours and 24 hours after seeding), or not treated as the control group. Neurite growth from the cut end of the CN was measured at 72 hours after seeding. The SCs from sciatic nerves were treated with MAP (0.033mJ/mm^2, 1 Hz, 100 pulses) twice (24 hours and 48 hours after seeding). After another 24 hours, the supernatant was collected to isolate exosomes, and cells were collected for reverse transcription polymerase chain reaction (RT-PCR) (Table 1) as previously reported[45–47].

To assess cell proliferation, SCs at passage 3–5 were plated onto 96-well plates at a density of 3×10^3 cells per well. Immediately after seeding, the cells were treated with MAP (0.033mJ/mm^2, 1 Hz, 100 pulses), and MTT (3-(4, 5-dimethylthiazolyl-2)-2, 5-diphenyltetrazolium bromide) cell proliferation assay was conducted at different timepoints to evaluate cellular viability. To assess the incorporation of EdU and H3P in SCs after MAP as indicators of cell proliferation, the cells were pulsed with 10uM EdU for 12 hours after seeding then treated with MAP (0.033mJ/mm2, 1 Hz, 100 pulses) and fixed 6 hours after treatment to measure the expression of H3p and EdU.

Exosome Isolation

To isolate exosomes, SCs at passage 3–5 were cultured in exosome-free medium prior to MAP treatment. After MAP treatment or control, exosomes were isolated from the SC culture medium by using Invitrogen™ Total Exosome Isolation Reagent (for cell culture media) (Thermo Fisher Scientific #4478359). In brief, the SC culture medium was collected and centrifuged at 2000 × g for 30 minutes then mixed with Total Exosome Isolation Reagent (0.5 volumes of culture medium) by vortex. After overnight incubation at 4°C, samples were centrifuged at 10,000 × g for 60 minutes at 4°C to obtain the total exosome pellet. The pellet was then resuspended in PBS and exosomes were confirmed by verifying exosome markers HSP70, HSP90 and CD63.

MPG Treated with Exosomes

After seeding in glass-covered six-well plates with Matrigel, MPG from 3 adult SD rats were cultured in different media according to experimental groupings (6 MPG fragments in each group). The control group was cultured with 3.0ml_ complete DMEM medium without FBS. The exosome-control (Exo-ctrl) group was cultured with 3.OmL complete DMEM medium with 500μL of exosomes isolated from SCs. The Exosome-MAP (Exo-MAP) group

was cultured with 3.OmL of complete DMEM medium with 500μL of exosomes isolated from SCs treated with MAP (0.033 mJ/mm^2, 1Hz, 100 pulses).

Neurite Growth Measurement

After 72 hours, neurite growth (including neurite length and number)from the MPG fragments was photographed at x50 with a Nikon DXM1200 digital still camera attached to a Zeiss Axiovert microscope using ACT-1 software (Nikon Instruments Inc.; Melville, NY, USA).

RT-PCR (Reverse Transcription-Polymerase Chain Reaction)

As previously reported[45–47], total RNA was extracted using the High Pure RNA Isolation Kit(Roche, Germany) following the kit instructions. Total RNA (2.5 μg) was annealed to 0.4 μg of oligo-dT primer in a volume of 12 μL. Then, 4 μL of 5× buffer, 2 μL of 0.1 mol/L Dithiothreitol (DTT), 1 μL of 10 mmol/LdNTP, and 1 μL of Super Script reverse transcriptase (Invitrogen, La Jolla, CA, USA) were added to bring the final volume to 20 μL. After 1 h of incubation at 42 °C, the mixture was incubated at 70 °C for 10 min to inactivate the reverse transcriptase. Then, 80 μL of Tris-EDTA (TE) buffer was added to make a 5× diluted complementary DNA library, from which 1 μL was used for RT-PCR. The cycling program was set for 35 cycles of 94 °C for 10 s, 55 °C for 10 s, and 72 °C for 10 s, followed by one cycle of 72 °C for 5 min. The PCR products were electrophoresed in 1.5% agarose gels, visualized by ultraviolet fluorescence, and recorded by a digital camera. Data were analyzed by ChemiImager-4000 software (Version 4.04, Alpha Innotech Corporation, San Leandro, CA, USA). Primer sequences are presented in Table 1.

Cell Proliferation Measurement

At 24, 48, 72, and 96 hours after seeding, cell proliferation was measured following the manual of CellTiter 96® AQueous (Promega, Madison, Wl) as previously reported. In brief, the CellTiter 96® AQueous One Solution Reagent was thawed in a water bath at 37°C. Atotal 20μl of CellTiter 96® AQueous One Solution Reagent was added to each well of the 96-well assay plate containing the cells in 100μl of culture medium and incubated at 37°C for 2 hours in 5% C02. Using the Emax precision microplate reader (Molecular Devices), the absorbance at 490nm was recorded and then converted into cell number.

Western Blot

The exosome protein samples were prepared in a lysis buffer containing 1% IGEPAL CA-630, 0.5% sodium deoxycholate, 0.1% sodium docecyl sulfate, aprotinin (10mg/mL), leupeptin (10mg/mL), and PBS. Exosome lysates containing 10μg of protein were electrophoresed in sodium docecyl sulfate polyacrylamide gel electrophoresis and then transferred to a polyvinylidene fluoride membrane (Millipore Corp; Bedford, MA, USA). The membrane was stained with Ponceau S to verify the integrity of the transferred proteins and to monitor the unbiased transfer of all protein samples. Detection of target proteins on the membranes was performed with an electrochemiluminescence kit (Amersham Life Sciences Inc; Arlington Heights, IL, USA) with the use of primary antibodies for HSP-70, HSP-90 (Abeam, 1:500), and CD63 (Santa Cruz Bio, 1:500). After the hybridization of

secondary antibodies, the resulting images were analyzed with Chemilmager 4000 (Alpha Innotec, Germany) to determine the integrated density value of each protein band.

Fluorescence Staining

Fluorescence staining was used to measure SC expression of S-100, MBP, H3P, and EdU as previously reported [48]. Briefly, SCs were incubated with primary antibodies, including S-100 (DAKO, 1:500), MBP (Abeam, 1:500), and H3P (EMD Millipore, 1:500), for 1 hour at room temperature. The cells were then incubated with Alexa Fluor-conjugated goat anti-rabbit or mouse antibody for 1 hour at room temperature. EdU was checked with Click-iT reaction cocktail conjugated with Alexa594-azide (EdU Click-iT Cat# C10339; Invitrogen) for 30min at room temperature. After nuclear staining with DAPI for 5min, the cells were examined under a fluorescence microscope and photographed.

Statistical Analysis

All experiments were repeated in triplicate, and all data were presented as the average of three independent experiments. Data were analyzed with Prism 5 (GraphPad Software; San Diego, CA) and presented as means ± standard deviation (S.D). Statistical significance between two groups was analyzed by the Student t-test. For statistical significance among multiple groups, one-way ANOVA analysis followed by Bonferroni post-hoc analysis was performed using the SAS software (SAS Institute Inc.; Cary, NC).

RESULTS

MAP Enhanced Neurite Outgrowth from MPG in a Dosage-Dependent Manner

First, we evaluated whether or not MAP influences neurite outgrowth (including length and number of neurites) of MPG *in vitro*. We found that 72 hours after treatment neurite outgrowth was enhanced by MAP (0.033 mJ/mm^2, 1Hz) in a dosage-dependent manner (Fig. 1a). The length of neurite outgrowth was measured (from the base of MPG to the end of neurite) and represented by polar graphs (Fig. 1b, c). The average length of neurite outgrowth was 300.8±19.7μm in the control group. This increased to 370.9±18.1μm ($P<0.05$), 460.5±21,9μm ($P<0.001$), 491,5±25.8μm ($P<0.001$), and 446.8±21,7μm ($P<0.001$) in the 25, 50, 100, and 200 pulse MAP treatment groups, respectively. Neurite outgrowth was only 336.7±19.4μm in the 300 pulse MAP treatment group (Fig. 1d). We also calculated the number of new neurites per mm of MPG tissue. In the control, the number of neurite was 28.0±1.6/mm. This increased to 36.6±1.8/mm ($P<0.01$), 43.9±1.1/mm ($P<0.0001$), 42.9±1.5/mm ($P<0.001$), and 35.7±1.0/mm ($P<0.01$) in the 25, 50, 100, and 200 pulse MAP treatment groups, respectively. Neurite number was only 29.9±1.3/mm in the 300 pulse MAP treatment group (Fig. 1 e). These findings indicate that low dosage MAP promotes MPG neurite outgrowth. This outgrowth peaks at 100 pulses but is diminished at the higher dosage of 300 pulses.

MAP Enhanced Neurite Outgrowth from CN/MPG

To investigate the effect of MAP on CN regeneration, we developed the *in vitro* model of CN/MPG culture. As shown in Figure 2b, we dissected the MPG with 2mm of CN attached and cultured the tissue *in vitro*. After 72 hours, new neurite outgrowth from the end of the

CN were measured. MAP (0.033 mJ/mm^2,1 Hz, 100 pulses) significantly improved the neurite outgrowth of CN (Fig. 3b). The average length of neurite outgrowth 72 hours after seeding was 372.5±13.7μm in the control and 555.8±17.3μm in the MAP treatment group (P<0.001) (Fig. 3c). The average number of neurites was 90.7±3.8/mm in the control and increased to 136.8±11.9/mm in the MAP treatment group (P<0.01) (Fig. 3d).

MAP Promoted SC Proliferation and Neurotropic Factor Expression

To investigate mechanisms by which MAP promotes neurite regeneration, SCs were isolated from the sciatic nerves of SD rats. SCs were confirmed by S100 and MBP through IF staining (Fig. 4a). Approximately 95% of the isolated cells were S100 positive, and 40% of the cells were both S100 and MBP positive. CellTiter 96® AQueous (Promega, Madison, Wl) was used to assay SC proliferation after MAP (0.033 mJ/mm^2, 1 Hz, 100 pulses) treatment. As shown in Fig. 4b, 24 hours after MAP treatment cell number was increased, but not significantly, as compared to the control. At timepoints of 48, 72, and 96 hours, the increase was significant (P < 0.05). The cell doubling time was then calculated; MAP reduced the SC doubling time from 54.1 ±1.5 hours to 46.9±3.50.9 hours (P < 0.05) (Fig. 4c). Next, we assessed whether MAP (0.033 mJ/mm^2, 1 Hz, 100 pulses) could promote H3P and EdU incorporation in SCs in vitro. As shown in Fig. 4d, the percentage of EdU incorporation was 51,49±4.12% in the control group, increasing to 67.79±3.51% (P < 0.05) in the MAP treatment group. The percentage of H3P positive cells was 2.77±0.59% in the control group, increasing to 7.86±1.24% (P < 0.01) in the MAP treatment group (Fig. 4e).

The impact of MAP (0.033 mJ/mm^2, 1 Hz, 100 pulses) on SC expression of neurotropic factors was assessed using RT-PCR *in vitro*. Neurotrophic factors, including BDNF (from 0.28±0.02 to 0.6±0.07; P<0.05), nerve growth factor (NGF) (from 0.84±0.07 to 1,54±0.22; P<0.05), and neurotrophin-3 (NT-3) (from 0.52±0.08 to 1.09±0.18; P<0.05), were up-regulated at the mRNA level after MAP treatment (Fig 4f).

MAP Enhanced SC Secretion of Exosomes, and SC-Derived Exosomes Promote MPG Neurite Outgrowth *In Vitro*

To assess whether MAP (0.033 mJ/mm^2,1 Hz, 100 pulses) treatment stimulates SCs to secrete exosomes, the SC culture medium was assayed for exosome proteins. The control SC exosome protein concentration was 0.41 ±0.08μg/μl. After MAP treatment the exosome protein concentration increased significantly to 1.22±0.06μg/μl (P<0.05) (Fig. s1a). To confirm that exosomes were successfully isolated, exosome markers including HSP-70, HSP-90 and CD63 were assessed by western blot. The exosomes isolated from both control SCs and MAP-treated SCs expressed HSP-70, HSP-90 and CD63 (Fig. s1b).

We further evaluated the effect of SC-derived exosomes on neurite outgrowth from MPG. Exosomes derived from SCs and exosomes derived from MAP (0.033 mJ/mm^2,1 Hz, 100 pulses) -treated SCs were added to the culture medium after MPG seeding (Fig. 5a). After 72 hours, the neurite outgrowth of MPG was enhanced (Fig. 5b). In the control group, the average length of neurite outgrowth was 311,6±23.9μm. In the SC-derived exosome group, the average length of neurite outgrowth increased significantly to 415.8±39.9μm (P<0.05). In the MAP-treated SC-derived exosome group, neurite outgrowth increased even further to

584.4±62.7μm (P<0.01). Moreover, the length of neurite outgrowth in the MAP-treated SCs-derived exosome group was significantly longer than in the SCs-derived exosome group (P<0.05) (Fig. 5c).

DISCUSSION

The prevalence of ED due to nerve damage after radical pelvic surgeries, such as prostatectomy or colectomy, is estimated to be between 14% and 90% [49]. Prostate cancer surgery including radical prostatectomy, may damage the cavernous nerve[50], leading to ED. Colectomy may damage the pelvic plexus or portions of the pudendal nerves or its branches, leading to similar consequences. Treatments focused on early stimulation of nerve regeneration after injury may encourage functional recovery, restoring erectile function prior to end organ atrophy and greatly benefitting patients.

In the past decades, Li-ESWT, a non-invasive mechano-biological intervention, has been proven to promote peripheral nerve regeneration [11,12] and has shown considerable promise as a treatment for neurogenic ED [17,18]. In this study, we investigated the potential for MAP, a similar but safer acoustic technology, to promote nerve regeneration. As early as 2003[41], we established an *ex vivo* ganglial culture system to study penile nerve regeneration after injury. In this study, we have utilized this model to demonstrate that MAP can promote pelvic nerve regeneration in a dosage response fashion. After 72 hours in culture, there was significant neurite outgrowth, both in the length and number, in the 25, 50, 100, and 200 pulse MAP-treated MPG groups (peak at 0.033 mJ/mm^2, 1Hz, 100pulses), compared with the control. However, the 300 pulse MAP-treated MPG group had no difference as compared to the control. This indicates that low dosage of MAP can promote nerve regeneration.

Recently, Dobbs, et al.[43] established the MPG/CN culture system to investigate the Sonic hedgehog (SHH) protein to the regeneration of injury cavernous nerve. To simulate nerve injury after prostate cancer surgery, we made some improvements to our previously described culture system according to the study of Dobbs, et al.[43]. In brief, in this study we cultured the whole MPG with the CN (CN/MPG). There are numerous neurite outgrowths from the CN, and this model better mimics the process of nerve regeneration after prostate cancer surgery as compared to our previous system. For studies in the field of neurogenic ED, this model provides an ideal alternative model as it makes single-factor studies easier to accomplish. As shown in our study employing this new CN/MPG culture system, the identified “ideal” dosage of MAP (0.033 mJ/mm^2, 1 Hz, 100pulses) was applied to treat the CN/MPG culture. After 72 hours of culturing, the neurites in the MAP-treated CN/MPG were much longer than in the control, which means that MAP promotes CN regeneration after injury.

Most fibers of the cavernous nerve (CN) are not myelinated, but rather are ensheathed into Remak bundles by non-myelinating SCs [21]. C fiber axons are grouped together into what is known as Remak bundles[51]. These occur when a non-myelinating Schwann cells bundles the axons close together by surrounding them. The Schwann cell keeps them from touching each other by squeezing its cytoplasm between the axons. Since we have shown that MAP can promote CN regeneration and that SCs are critical for nerve regeneration, primary SCs were

isolated from SD rat sciatic nerve to further investigate the mechanisms of MAP. After isolation, SCs were identified by S-100 (marker for SCs) and MBP (marker for myelinating SCs) through IF staining. Results confirmed that the cells isolated were mostly SCs and among them 40% of them were myelinating SCs and the rest were non-myelinating SCs.

Previous studies have proven that Li-ESWT can promote peripheral nerve regeneration through the activation of SCs and by stimulating SCs to secrete neurotropic factors[11,12]. In this study, we evaluated whether MAP may have similar effects on SCs. As shown in Figure.4, MAP significantly reduced cell doubling time, increased cell number, and increased the percentage of EdU- or H3P (phosphorylated histone 3)- positive SCs. This means that MAP promoted SC proliferation. In addition, we found that MAP increased the expression of neurotropic factors, including BDNF, NGF, and NT-3. This suggests that MAP can promote cell survival in addition to stimulating nerve regenerating[20]. Overall, these results indicate that MAP has similar mechanisms to Li-ESWT in promoting nerve regeneration.

Very recently, it was reported that SCs regulate peripheral nerve regeneration by secreting exosomes[32–34]. Exosomes containing mRNA, miRNA, and protein cargos can promote axonal regeneration after peripheral nerve injury. Secreted by SCs in exosomes, miRNA340 can promote debris clearance following nerve crush injury. In addition, dysregulation of miRNA340 expression alters cell debris removal and axonal regeneration[52]. Yu *et al*[53] also reported significant expression changes of 77 miRNAs in the proximal nerve stump following rat sciatic nerve injury. Moreover, upregulation of miR-221 and miR-222 cluster (miR-221/222) was found to promote SC proliferation and migration by modulating SC phenotype. In our study, we found that SC-derived exosomes with or without MAP treatment promoted nerve regeneration *in vitro*. Notably, the secretion of exosomes from SCs was significantly increased after MAP treatment, and MAP-treated SC-derived exosomes had a greater impact on nerve regeneration than exosomes derived from non-MAP treated SCs.

In this study, MAP treatment significantly increased SC proliferation, which partially explains the promotion of exosome secretion and the increased neurotrophic factor expression. MAP, a mechanical force, also promoted the synthesis and secretion of exosomes from SCs.

It should be cautioned that our study has limitations and that our findings require further validation. In our study, 12 weeks old SD rats were used to obtain better results as we know that nerve regeneration is more robust in the younger rats. For the next step, elderly SD rats will be used to test the relevant effects. Our study did not explore the exact mechanisms through which MAP induces SCs to secrete exosomes nor did it explore whether or not MAP regulates the content of the exosomes. In addition, SCs from myelinated sciatic nerve, not the non-myelinated cavernous nerve, were used for the experiment. Further study with SCs from the cavernous nerve will be needed to prove the hypothesis.

CONCLUSION

In this study, we used the *ex vivo* culture of MPG with CN for the study of nerve regeneration. Furthermore, we confirmed that MAP treatment facilitates nerve regeneration by promoting SC proliferation, by increasing NF expression (BDNF, NGF and NT-3), and by stimulating SC to secrete exosomes.

Supplementary Material

Refer to Web version on PubMed Central for supplementary material.

ACKNOWLEDGMENTS

Research reported in this publication was supported by NIDDK of the National Institutes of Health under award number R56DK105097 and 1R01DK105097-01A1. It was also supported by Army, Navy, NIH, Air Force, VA and Health Affairs to support the AFIRM II effort, under Award number W81XWH-13-2-0052. Opinions, interpretations, conclusions, and recommendations are those of the author and are not necessarily endorsed by the Department of Defense and do not necessarily represent the official views of the National Institutes of Health.

REFERENCES

[1]. Calabro RS, Polimeni G, Bramanti P. Recent advances in the treatment of neurogenic erectile dysfunction. Recent Pat CNS Drug Discov. 2014;9: 41–53. [PubMed: 24483711]

[2]. Ciaramitaro P, Mondelli M, Logullo F, et al. Traumatic peripheral nerve injuries: epidemiological findings, neuropathic pain and quality of life in 158 patients. J Peripher Nerv Syst 2010;15: 120–7. [PubMed: 20626775]

[3]. Torres RY, Miranda GE. Epidemiology of Traumatic Peripheral Nerve Injuries Evaluated by Electrodiagnostic Studies in a Tertiary Care Hospital Clinic. Bol Asoc Med P R 2015;107: 79–84. [PubMed: 26742202]

[4]. Hatzichristou D, d'Anzeo G, Porst H, et al. Tadalafil 5 mg once daily for the treatment of erectile dysfunction during a 6-month observational study (EDATE): impact of patient characteristics and comorbidities. BMC Urol 2015;15: 111. [PubMed: 26563171]

[5]. Rusovan A, Kanje M. Magnetic fields stimulate peripheral nerve regeneration in hypophysectiomized rats. Neuroreport. 1992;3:1039–41. [PubMed: 1493213]

[6]. Sene GA, Sousa FF, Fazan VS. Barbieri CH. Effects of laser therapy in peripheral nerve regeneration. Acta Ortop Bras 2013;21; 266–70.

[7]. Elzinga K, Tyreman N, Ladak A, Savaryn B, Olson J, Gordon T. Brief electrical stimulation improves nerve regeneration after delayed repair in Sprague Dawley rats. Exp Neurol. 2015;269: 142–53. [PubMed: 25842267]

[8]. Ma F, Xiao Z, Chen B, Hou X, Dai J, Xu R. Linear ordered collagen scaffolds loaded with collagen-binding basic fibroblast growth factor facilitate recovery of sciatic nerve injury in rats. Tissue Eng Part A. 2014;20:1253–62. [PubMed: 24188561]

[9]. Montava M, Garcia S, Mancini J, et al. Vitamin D3 potentiates myelination and recovery after facial nerve injury. Eur Arch Otorhinolaryngol. 2015;272: 2815–23. [PubMed: 25261104]

[10]. Wang Y, Shen W, Yang L, Zhao H, Gu W, Yuan Y. The protective effects of Achyranthes bidentata polypeptides on rat sciatic nerve crush injury causes modulation of neurotrophic factors. Neurochem Res. 2013;38: 538–46. [PubMed: 23242788]

[11]. Hausner T, Pajer K, Halat G, et al. Improved rate of peripheral nerve regeneration induced by extracorporeal shock wave treatment in the rat. Exp Neurol. 2012;236: 363–70. [PubMed: 22575596]

[12]. Hausner T, Nogradi A. The use of shock waves in peripheral nerve regeneration: new perspectives? Int Rev Neurobiol 2013;109: 85–98. [PubMed: 24093607]

[13]. Gruenwald I, Appel B, Vardi Y. Low-intensity extracorporeal shock wave therapy-a novel effective treatment for erectile dysfunction in severe ED patients who respond poorly to PDE5 inhibitor therapy. J Sex Med 2012;9: 259–64. [PubMed: 22008059]

[14]. Lu Z, Lin G, Reed-Maldonado A, Wang C, Lee YC, Lue TF. Low-intensity Extracorporeal Shock Wave Treatment Improves Erectile Function: A Systematic Review and Meta-analysis. Eur Urol 2017;71: 223–33. [PubMed: 27321373]

[15]. Vardi Y, Appel B, Jacob G, Massarwi O, Gruenwald I. Can low-intensity extracorporeal shockwave therapy improve erectile function? A 6-month follow-up pilot study in patients with organic erectile dysfunction. Eur Urol 2010;58: 243–8. [PubMed: 20451317]

[16]. Vardi Y, Appel B, Kilchevsky A, Gruenwald I. Does low intensity extracorporeal shock wave therapy have a physiological effect on erectile function? Short-term results of a randomized, double-blind, sham controlled study. J Urol. 2012;187: 1769–75. [PubMed: 22425129]

[17]. Zou ZJ, Liang JY, Liu ZH, Gao R, Lu YP. Low-intensity extracorporeal shock wave therapy for erectile dysfunction after radical prostatectomy: a review of preclinical studies. Int J Impot Res. 2018;30: 1–7. [PubMed: 29180799]

[18]. Frey A, Sonksen J, Fode M. Low-intensity extracorporeal shockwave therapy in the treatment of postprostatectomy erectile dysfunction: a pilot study. Scand J Urol. 2016;50: 123–7. [PubMed: 26493542]

[19]. Li H, Matheu MP, Sun F, et al. Low-energy Shock Wave Therapy Ameliorates Erectile Dysfunction in a Pelvic Neurovascular Injuries Rat Model. J Sex Med 2016;13: 22–32. [PubMed: 26755082]

[20]. Caillaud M, Richard L, Vallat JM, Desmouliere A, Billet F. Peripheral nerve regeneration and intraneural revascularization. Neural Regen Res. 2019;14: 24–33. [PubMed: 30531065]

[21]. Schaumburg HH, Zotova E, Cannella B, et al. Structural and functional investigations of the murine cavernosal nerve: a model system for serial spatio-temporal study of autonomic neuropathy. BJU Int. 2007;99: 916–24. [PubMed: 17378850]

[22]. Reichert F, Saada A, Rotshenker S. Peripheral nerve injury induces Schwann cells to express two macrophage phenotypes: phagocytosis and the galactose-specific lectin MAC-2. J Neurosci. 1994;14: 3231–45. [PubMed: 8182468]

[23]. Ronchi G, Nicolino S, Raimondo S, et al. Functional and morphological assessment of a standardized crush injury of the rat median nerve. J Neurosci Methods. 2009;179: 51–7. [PubMed: 19428511]

[24]. Vrbova G, Mehra N, Shanmuganathan H, Tyreman N, Schachner M, Gordon T. Chemical communication between regenerating motor axons and Schwann cells in the growth pathway. Eur J Neurosci. 2009;30: 366–75. [PubMed: 19656172]

[25]. Rath EM, Kelly D, Bouldin TW, Popko B. Impaired peripheral nerve regeneration in a mutant strain of mice (Enr) with a Schwann cell defect. J Neurosci. 1995;15: 7226–37. [PubMed: 7472477]

[26]. Webber C, Zochodne D. The nerve regenerative microenvironment: early behavior and partnership of axons and Schwann cells. Exp Neurol. 2010;223: 51–9. [PubMed: 19501085]

[27]. Toews AD, Barrett C, Morell P. Monocyte chemoattractant protein 1 is responsible for macrophage recruitment following injury to sciatic nerve. J Neurosci Res. 1998;53: 260–7. [PubMed: 9671983]

[28]. Klein D, Martini R. Myelin and macrophages in the PNS: An intimate relationship in trauma and disease. Brain Res. 2016;1641:130–38. [PubMed: 26631844]

[29]. Fu SY, Gordon T. The cellular and molecular basis of peripheral nerve regeneration. Mol Neurobiol. 1997;14: 67–116. [PubMed: 9170101]

[30]. Lin G, Zhang H, Sun F, et al. Brain-derived neurotrophic factor promotes nerve regeneration by activating the JAK/STAT pathway in Schwann cells. Translational andrology and urology 2016;5: 167–75. [PubMed: 27141442]

[31]. Wang B, Ning H, Reed-Maldonado AB, et al. Low-Intensity Extracorporeal Shock Wave Therapy Enhances Brain-Derived Neurotrophic Factor Expression through PERK/ATF4 Signaling Pathway. International journal of molecular sciences. 2017;18.

[32]. Qing L, Chen H, Tang J, Jia X. Exosomes and Their MicroRNA Cargo: New Players in Peripheral Nerve Regeneration. Neurorehabil Neural Repair. 2018;32: 765–76. [PubMed: 30223738]

[33]. Lopez-Leal R, Court FA. Schwann Cell Exosomes Mediate Neuron-Glia Communication and Enhance Axonal Regeneration. Cell Mol Neurobiol. 2016;36: 429–36. [PubMed: 26993502]

[34]. Lopez-Verrilli MA, Picou F, Court FA. Schwann cell-derived exosomes enhance axonal regeneration in the peripheral nervous system. Glia. 2013;61: 1795–806. [PubMed: 24038411]

[35]. Thery C, Ostrowski M, Segura E. Membrane vesicles as conveyors of immune responses. Nat Rev Immunol. 2009;9: 581–93. [PubMed: 19498381]

[36]. Shao H, Im H, Castro CM, Breakefield X, Weissleder R, Lee H. New Technologies for Analysis of Extracellular Vesicles. Chemical Reviews. 2018;118: 1917–50. [PubMed: 29384376]

[37]. Qiu X, Lin G, Xin Z, et al. Effects of low-energy shockwave therapy on the erectile function and tissue of a diabetic rat model. The journal of sexual medicine. 2013;10: 738–46. [PubMed: 23253086]

[38]. Ruan Y, Zhou J, Kang N, et al. The effect of low-intensity extracorporeal shockwave therapy in an obesity-associated erectile dysfunction rat model. BJU international 2018;122: 133–42. [PubMed: 29573106]

[39]. Lin G, Reed-Maldonado AB, Wang B, et al. In Situ Activation of Penile Progenitor Cells With Low-Intensity Extracorporeal Shockwave Therapy. J Sex Med 2017;14: 493–501. [PubMed: 28258952]

[40]. Peng D, Yuan H, Liu T, et al. Smooth Muscle Differentiation of Penile Stem/Progenitor Cells Induced by Microenergy Acoustic Pulses In Vitro. J Sex Med 2019.

[41]. Lin G, Chen KC, Hsieh PS, Yeh CH, Lue TF, Lin CS. Neurotrophic effects of vascular endothelial growth factor and neurotrophins on cultured major pelvic ganglia. BJU Int. 2003;92: 631–5. [PubMed: 14511050]

[42]. Lin G, Shindel AW, Fandel TM, Bella AJ, Lin CS, Lue TF. Neurotrophic effects of brain-derived neurotrophic factor and vascular endothelial growth factor in major pelvic ganglia of young and aged rats. BJU international 2010;105: 114–20. [PubMed: 19493269]

[43]. Dobbs R, Kalmanek E, Choe S, et al. Sonic hedgehog regulation of cavernous nerve regeneration and neurite formation in aged pelvic plexus. Exp Neurol. 2019;312: 10–19. [PubMed: 30391523]

[44]. Wilby MJ, Muir EM, Fok-Seang J, Gour BJ, Blaschuk OW, Fawcett JW. N-Cadherin inhibits Schwann cell migration on astrocytes. Mol Cell Neurosci. 1999;14: 66–84. [PubMed: 10433818]

[45]. Lin G, Xin Z, Zhang H, et al. Identification of active and quiescent adipose vascular stromal cells. Cytotherapy. 2012;14: 240–6. [PubMed: 22070603]

[46]. Lin G, Wang G, Banie L, et al. Treatment of stress urinary incontinence with adipose tissue-derived stem cells. Cytotherapy. 2010;12: 88–95. [PubMed: 19878076]

[47]. Lin G, Shindel AW, Banie L, et al. Molecular mechanisms related to parturition-induced stress urinary incontinence. European urology. 2009;55: 1213–22. [PubMed: 18372098]

[48]. Lin G, Huang YC, Shindel AW, et al. Labeling and tracking of mesenchymal stromal cells with EdU. Cytotherapy 2009;11: 864–73. [PubMed: 19903099]

[49]. Salonia A, Castagna G, Capogrosso P, Castiglione F, Briganti A, Montorsi F. Prevention and management of post prostatectomy erectile dysfunction. Transl Androl Urol. 2015;4: 421–37. [PubMed: 26816841]

[50]. Tal R, Alphs HH, Krebs P, Nelson CJ, Mulhall JP. Erectile function recovery rate after radical prostatectomy: a meta-analysis. J Sex Med. 2009;6: 2538–46. [PubMed: 19515209]

[51]. Murinson BB, Griffin JW. C-fiber structure varies with location in peripheral nerve. J Neuropathol Exp Neurol. 2004;63: 246–54. [PubMed: 15055448]

[52]. Li S, Zhang R, Yuan Y, et al. MiR-340 Regulates Fibrinolysis and Axon Regrowth Following Sciatic Nerve Injury. Mol Neurobiol. 2017;54: 4379–89. [PubMed: 27344331]

[53]. Yu B, Zhou S, Wang Y, et al. miR-221 and miR-222 promote Schwann cell proliferation and migration by targeting LASS2 after sciatic nerve injury. J Cell Sci. 2012;125: 2675–83. [PubMed: 22393241]

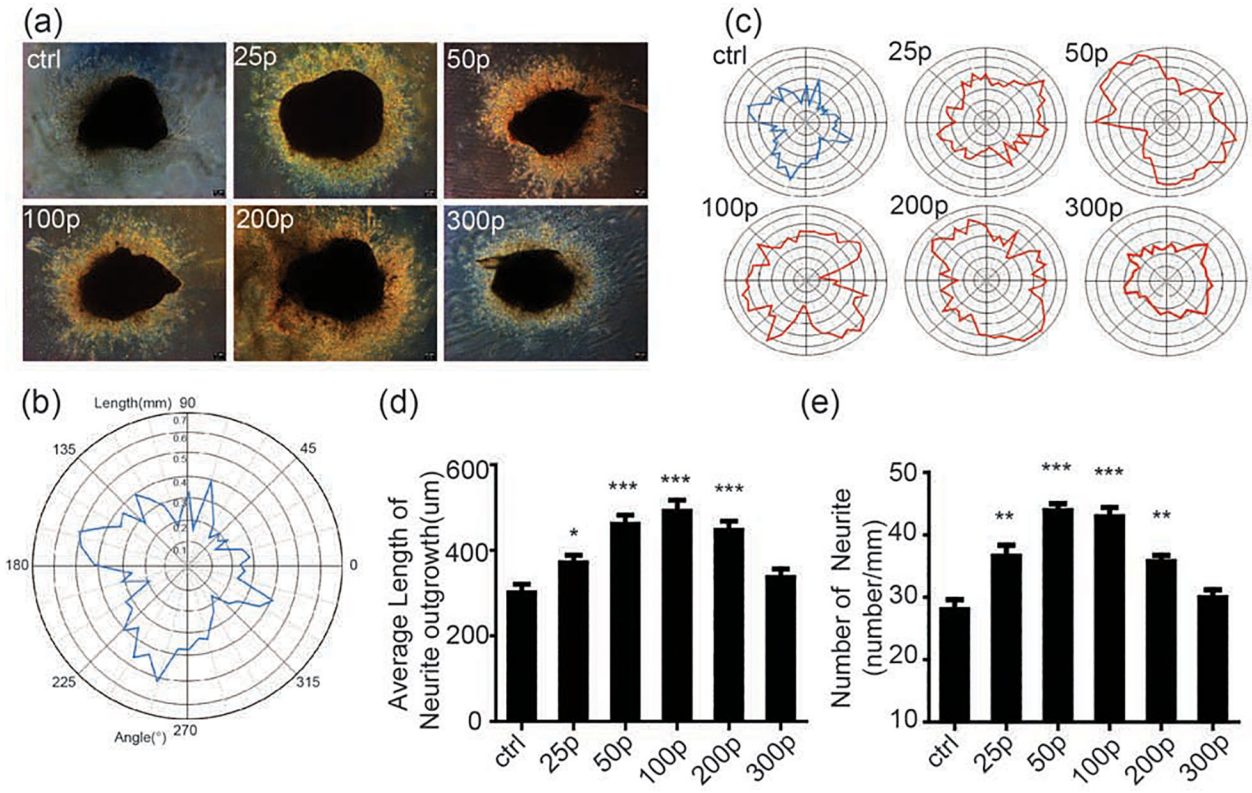

Figure 1. MAP enhanced neurite outgrowth from MPG in a dosage response manner *in vitro*.

(a). Neurite outgrowth from MPG after different dosages of MAP (0.033 mJ/mm^2, 1Hz, 25/50/100/200/300 pulses). Original magnification x50. The arrow indicates fiber outgrowth, (b). Polar graphs were used to represent the average shape of the outgrowing fibers from MPG. (c). Polar graphs of all groups, (d). MAP promoted outgrowth of MPG fibers in a dosage response manner, and fiber outgrowth peaked at 100 pulses, (e). MAP promoted the number of MPG fibers in a dosage response manner. (n=6, Error bars represent SD, *P< 0.05, **P< 0.01,***P< 0.001).

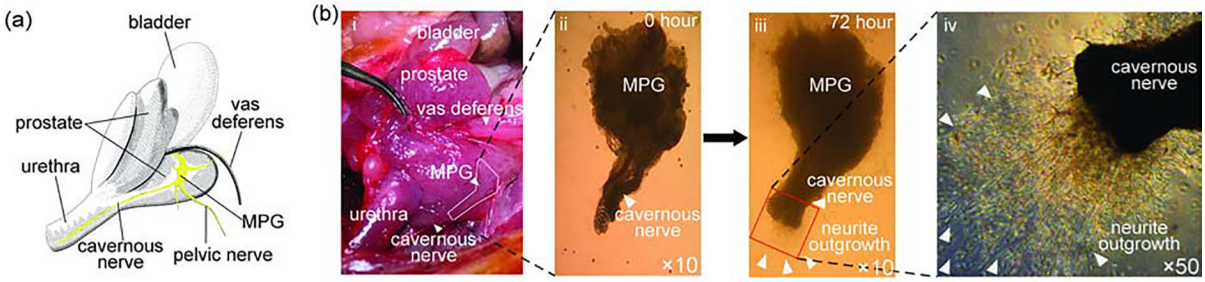

Figure 2. Schematic diagram of MPG/CN culture.

(a). Anatomy of MPG/CN. (b). i. MPG/CN of SD rats were dissected and exposed; ii. MPG/CN (2mm of CN) were seeded onto the glass and covered with Matri-gel; iii. After 72 hours in culture, the fibers were growing from the CN endings; iv. Higher power (x50) to show the fiber outgrowths.

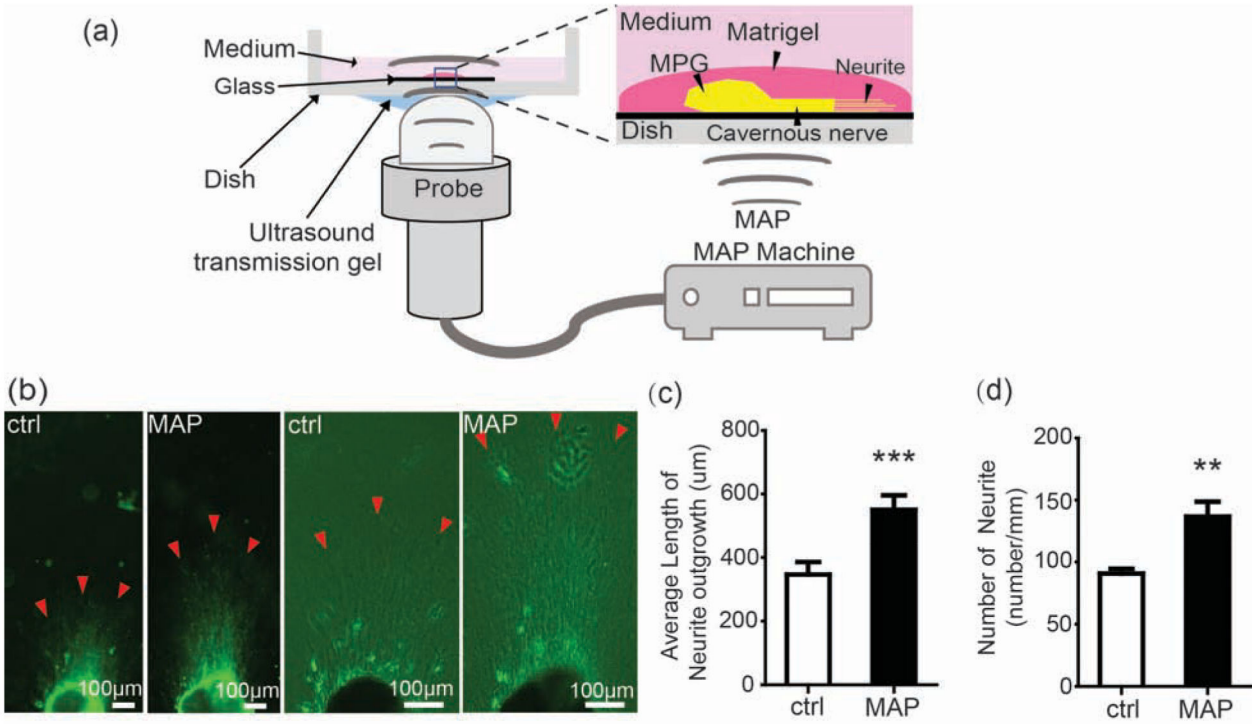

Figure 3. MAP enhanced neurite outgrowth from CN *in vitro*.

(a). Schematic diagram to show MAP-treated MPG/CN. (b). Neurite outgrowth from CN 72 hours after seeding. Original magnification x50 (left two) and x100 (right two). The red arrow indicates outgrowing fibers, (c). MAP (0.033 mJ/mm^2, 1 Hz, 100 pulses) promoted fiber outgrowth from CN. (d). MAP promoted the number of fibers from CN. (n=6, Error bars represent SD, **P< 0.01, ***p< 0.001).

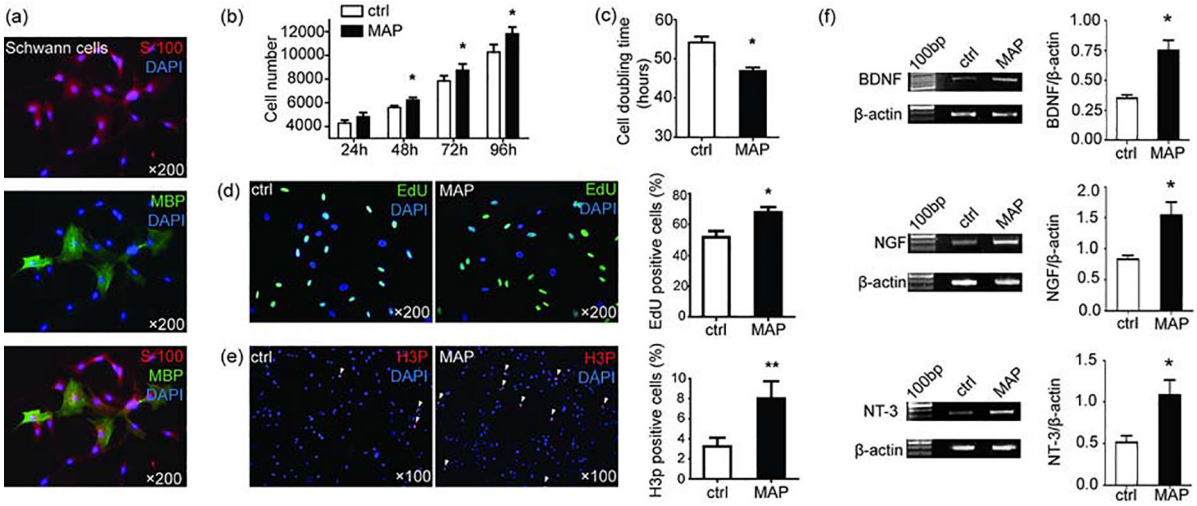

Figure 4. MAP promoted SC proliferation and SC neurotrophic factor expression.

(a). IF staining showing that SCs were S100 and MBP positive, (b). Twenty-four hours after MAP, more EdU-positive cells were noted with IF staining in the MAP (0.033 mJ/mm^2, 1 Hz, 100 pulses) group, (c). Twenty-four hours after MAP, more H3P-positive cells were noted with in the MAP (0.033 mJ/mm^2, 1Hz, 100 pulses) group, (d). Twenty-four hours after MAP (0.033 mJ/mm^2, 1Hz, 100 pulses), expression of NFs, including BDNF, NGF and NT-3, was upregulated at the mRNA level in the MAP group. (n=3, Error bars represent SD, *P< 0.05, **P< 0.01).

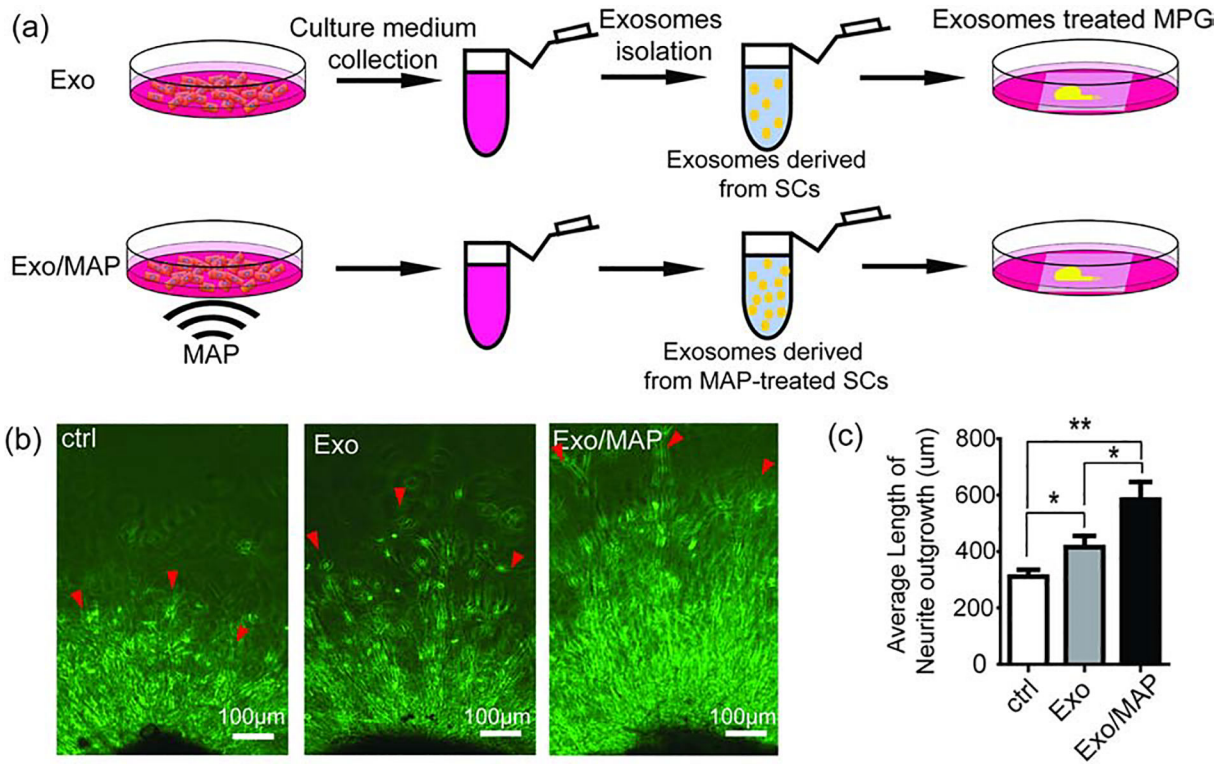

Figure 5. SC-derived exosomes enhanced neurite outgrowth from MPG *in vitro*.

(a). Schematic diagram of exosome isolation and MPG treated with exosomes. (b). Neurite outgrowth from MPG 72 hours after SCs-derived exosome treatment. Original magnification x100. The red arrow indicates outgrowing fibers, (c). SC-derived exosomes and MAP-treated SC-derived exosomes promoted neurite outgrowth, and MAP (0.033 mJ/mm^2, 1Hz, 100 pulses)-treated SCs-derived exosomes had a better effect. (n=6, Error bars represent SD, *P< 0.05, **P< 0.01).

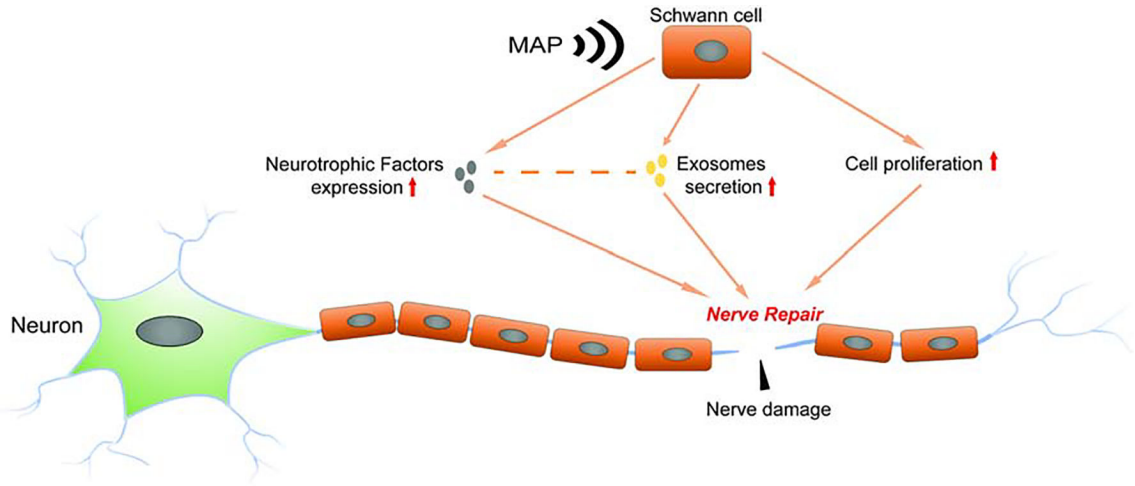

Figure 6.
Schematic representation of the proposed mechanisms by which MAP promotes nerve regeneration.

Table 1.

Reverse Transcription-PCR primer sequences

Gene	Forward	Reverse
β-actin	CTACAATGAGCTGCGTGTG	AATGTCACGCACGATTTCCC
BDNF	ACTT CGGTT GCAT GAAGGCT	G GT CAGT GTACATACACAGG
NGF	AACAGGACT CACAGGAGGAA	CTTCCTGCT GAGCACACACA
NT-3	GAGCATAAGAGTCACCGAGG	GACAAGGCACACACACAGGA